Nanoparticles Incorporated in Bilaminated Films: A Smart Drug Delivery System for Oral Formulations

Fuying Cui,[†,‡] Chunbai He,[†,‡] Lichen Yin,[†] Feng Qian,[†,‡] Miao He,[†,‡] Cui Tang,[†] and Chunhua Yin*[,†]

State Key Laboratory of Genetic Engineering, Department of Pharmaceutical Sciences, School of Life Sciences, Fudan University, Shanghai 200433, China, and Department of Biochemistry, School of Life Sciences, Fudan University, Shanghai 200433, China

Received March 26, 2007; Revised Manuscript Received June 16, 2007

A novel smart drug delivery system (NP-Film) consisting of carboxylation chitosan-grafted nanoparticles (CCGNs) and bilaminated films, which were composed of the mucoadhesive chitosan−ethylenediaminetetraacetic acid hydrogel layer and the hydrophobic ethylcellulose layer, was developed for oral delivery of protein drugs. NP-Film was characterized by electron microscopy and fluorescence microscopy, and the results showed that the solid, spherical nanoparticles dispersed evenly in the porous structures of films. The properties of nanoparticles and films were investigated. The mucoadhesive force, CCGNs released from the NP-Film, and the toxicity of NP-Film were also evaluated. Results showed that the nanoparticles could reversibly open the tight junction of the intestine and inhibit trypsin activity. The release behavior of the nanoparticles from the NP-Film exhibited pH sensitivity. The drug delivery system possessed high mucoadhesive force and low intestinal toxicity. Therefore, the NP-Film would be a promising delivery carrier for protein drugs via oral administration.

Introduction

Oral administration is a noninvasive route of drug delivery. However, peptide and protein drug delivery through the gastrointestinal (GI) tract remains a highly challenging task because of their low bioavailability resulting from the pH fluctuation, proteolytic degradation, low transport efficiency, and short residence time.[1,2]

Mucoadhesive drug delivery systems have attracted considerable interest because of their sustained drug release profile at the absorption site and increasing drug bioavailability due to the intimate contact with the absorbing tissue. Recently, several research groups have made efforts to design patch-like asymmetric delivery devices with functionalities such as mucoadhesion, drug protection, and targeted unidirectional release.[3,4]

Another strategy includes the use of liposomes, microparticles, and nanoparticles. The drug carrier systems administered to mucosal surfaces may protect drugs from degradation during the passage through the GI tract, enhance the uptake by the epithelium, and act as a controlled release system resulting in prolonged blood concentrations.[5]

A good candidate seems to combine the advantages of the two approaches. Thus, the NP-Film was designed by carboxylation chitosan-grafted nanoparticles (CCGNs) incorporating physically into chitosan−ethylenediaminetetraacetic acid hydrogels (Ch-EA) of the bilaminated film. The NP-Film was characterized by electron microscopy and fluorescence microscopy. The encapsulation efficiency for hydrophilic proteins such as insulin, the effect on the intestinal membrane resistance, the stability in simulated GI conditions, and the enzymatic inhibition of nanoparticles were evaluated. The swelling behavior of the bilaminated film was investigated. The mucoadhesive force, the toxicity of the NP-Film, and the CCGNs released from it were also evaluated.

* Corresponding author. Tel: +86-21-65643797. Fax: +86-21-55522771. E-mail address: chyin@fudan.edu.cn.

[†] Department of Pharmaceutical Sciences.

[‡] Department of Biochemistry.

Experimental Section

Materials. Chitosan hydrochloride (Ch) with a degree of deacetylation of approximately 86.5% was supplied by Yuhuan Ocean Biochemistry Co., Ltd. (Zhejiang, China). Carboxylation chitosan with a substitution of the carboxyl group above 60% was also supplied by Yuhuan Ocean Biochemistry Co., Ltd. Methyl methacrylate (M_w = 100.12) and ammonium persulfate (APS, M_w = 228.20) were purchased from Lingfeng Chemical Co. (Shanghai, China) and Anjian Chemical Co. (Shanghai, China), respectively. Insulin (27.6 IU/mg) was purchased from Xuzhou biochemical plant (Jiangsu, China). 1-Ethyl-3-(3-dimethylaminopropyl) carbodiimide hydrochloride (EDAC, M_w = 191.70) was purchased from Shanghai Sanjie Biotechnology Co., Ltd. Ethylenediaminetetraacetic acid disodium salt (Na_2-EDTA, M_w = 372.24) was purchased from Shanghai Chemical Reagent Co., Ltd. Ethylcellulose (EC) was purchased from the Institute of Pharmaceutical Industry (Shanghai, China). Coumarin-6 was kindly supplied by the School of Pharmacy, Fudan University. Trypsin was obtained from Bo'ao Chemical Co., (Shanghai, China). Male Sprague−Dawley strain rats of 200−250 g weight were provided by the Animal Center Care Center, Fudan University. The study protocol was reviewed and approved by the Institutional Animal Care and Use Committee, Fudan University, China.

Preparation of CCGNs. CCGNs were prepared according to our previous methods.[6] Briefly, carboxylation chitosan was dissolved in water under magnetic stirring. The monomer methyl methacrylate was dissolved in the above mixture at 75 °C. Thereafter, APS solution was added. The reaction was completed after 24 h. Different batches were prepared according to the following reaction conditions:

(1) The concentration of the initiator APS was varied between 0.01 and 0.05% (w/v).

(2) Ratios of carboxylation chitosan to methyl methacrylate were varied while the total monomer content and the concentration of the initiator APS were kept constant.

10.1021/bm070339e CCC: $37.00
Published on Web 08/01/2007

Poly(methyl methacrylate) (PMMA) nanoparticles were prepared as carboxylation chitosan was not added. These stock suspensions were purified by dialysis through a semipermeable membrane with an exclusion size of 14 000 Da (Green Bird Science Development Limited Company, Shanghai, China), lyophilized.

The freeze-dried nanoparticles were suspended in water, while coumarin-6 was dissolved in ethanol. They were mixed together for 1 h. The labeled nanoparticles were collected by centrifugation (15 000 rpm, 40 min), washed with water 3 times to remove excessive coumarin-6, then lyophilized.

Preparation of the Mucoadhesive Layer: Ch-EA Hydrogels. Ch-EA hydrogels were synthesized in a modified way as described previously by Bernkop-Schnürch et al.[7] A 0.1 g portion of Ch was dissolved in 8 mL of water. Na_2-EDTA was added in the solution. Then, EDAC was added to the reaction to reach a final concentration of 0.01 M. The reaction mixture was incubated for 4 h at room temperature under stirring.

Preparation of the Hydrophobic Backing Layer: EC Layer. The backing layer was prepared by the solvent casting method. A 0.3 g portion of EC was dissolved in 6 mL of ethanol, into which 0.06 g of glycerin was added, thus obtaining the plasticized EC solution (5%, w/v). The plasticized EC was cast in a circular dish of 28 cm^2, and the solvent was evaporated at room temperature. This procedure produced an EC layer of about 8 μm in thickness.

Preparation of the NP-Film. The freeze-dried nanoparticles were added into Ch-EA, and the mixture was stirred for 1 h. The yielding hydrogel was cast onto the dried backing layer. The dish was stored at 4 °C for 24 h to remove all the air bubbles entrapped and then dried under vacuum. The NP-Film was carefully peeled off and stored at room temperature in a desiccator. The bilaminated film was prepared as the freeze-dried nanoparticles were not added.

Preparation of Capsules Containing the NP-Film. The NP-Film was divided into small films (6×6 mm^2). They were encapsulated into enteric coated capsules.

Morphology. Images of capsules containing the NP-Film were photographed. Transmission electron microscopy (TEM) was used to observe the morphology of the CCGNs. Samples were immobilized on copper grids and negatively stained with phosphotungstic acid. After being dried at room temperature, they were examined by TEM (Hitachi, Japan). The morphological characteristics of the NP-Film were coated with a thin layer of palladium gold alloy and imaged by scanning electron microscopy (SEM). Coumarin-6-labeled nanoparticles dispersed in the NP-Film were also observed by a fluorescence microscope.

Particle Size and Zeta Potential of Nanoparticles. The particle size and the polydispersity index (PDI) of the resulting nanoparticles were determined by photon correlation spectroscopy with a BI 90 particle sizer (Brookhaven Instruments Corp., Holtsville, NY). Each sample diluted with double distilled water was measured, and the value was reported.

The zeta potential of each nanoparticle formulation was determined by microelectrophoresis with a Zeta Plus, zeta potential analyzer (Brookhaven Instruments). The zeta potential was measured by diluting a sample with double-distilled water.

Encapsulation Efficiency. Insulin dissolved in 0.01 N hydrochloride acid was mixed with CCGN colloids. The mixture was stirred gently with a magnetic stirrer at room temperature for 1 h. Each mixture was centrifuged at 15 000 rpm for 40 min at 4 °C to separate the free drug in the supernatant from the drug incorporated in the nanoparticles. The concentrations of insulin in the supernatant were determined by the Lowry Reaction method[8] and by visible spectrometry at 750 nm. The encapsulation efficiency was calculated as $(A - B)/A \times 100\%$, where A is the total amount of insulin and B is the amount of non-loaded insulin in the supernatant.[9,10]

Effects on the Tight Junctions.[9] Overnight-fasted male Sprague−Dawley rats (200−250 g) were euthanized by exsanguination through cutting the carotid artery under ether anesthesia. The ileum was removed, cut longitudinally, and then set into the diffusion-type Ussing chamber. Both serosal and mucosal sides of the intestine were washed with 5 mL of Krebs−Ringer solution (pH 7.4, bubbled with O_2/CO_2, 95:5). After exchange of Krebs−Ringer solution, electrodes were fixed at both sides. Membrane resistance (R_m) was measured after 10 min preincubation. Thereafter, 0.5 mL of CCGN colloids was added to the Krebs−Ringer solution on the mucosal side. Every 10 min within 30 min after adding nanoparticles, R_m was measured again, and its difference induced by nanoparticles was calculated. As a positive control, 0.5 mL of sodium tauroglycocholate (STG) aqueous solution (10 mg/mL) was added to the Krebs−Ringer solution. Double-distilled water was used as the negative control.

Enzyme Inhibition. Trypsin was incubated in a borate-buffered solution under pH 7.5, either in the presence or in the absence of nanoparticles at 37 °C for 20 min, respectively. The initial concentration of nanoparticles was 10 mg/mL, and the activity of trypsin was 1500 BAEE U/mg. The detailed method for trypsin inhibition activity was according to our previous studies.[11]

Stability of Nanoparticles in Simulated GI Conditions. The freeze-dried coumarin-6-labeled CCGNs were incubated in a simulated gastric medium (pH 1.2) and an intestinal medium (pH 7.4) for 1 h. Their morphological changes were characterized by fluorescence microscope.

Swelling Behavior of the Bilaminated Film. The swelling characteristics of the bilaminated film were determined by immersing dried test samples to swell in solutions with different pH values and ionic strengths at room temperature. At timed intervals, samples were removed from solutions and weighed after excess solutions on the surfaces were blotted. The swelling ratios (Q_s) of the film were calculated from the following expression:

$$Q_s = (W_s - W_d)/W_d$$

where W_d is the weight of the dry film, and W_s is the weight of the swollen film at certain time intervals.

In Vitro Mucoadhesive Force. The mucoadhesive force was determined by a modified precision torsion balance (Shanghai Precision Science Instrument Limited Co., 2500 mg/5 mg). The NP-Film and bilaminated film were fixed to the upper support, and a section of intestine was attached to the lower rubber support with the mucosal side up. The procedure was in accordance with the work of Yin et al.[12] The force per unit area required to detach the test film from the biological substrate in the present study was calculated from the equation

$$F = W \cdot G/A$$

where F represents the mucoadhesive force (N/m^2); W is the maximum detachment weight recorded by the balance (kg); G is acceleration due to gravity (ms^{-2}); A is the film−tissue contact area (m^2).

Release of Nanoparticles from the NP-Film. Nanoparticles released from the NP-Film were carried out in the simulated gastric medium for 2 h and in the intestinal medium for another 5 h and stirred at 100 rpm. A 0.5 mL portion of the samples was collected at predetermined time intervals and replaced with an equal volume of fresh release medium. Nanoparticle concentrations in each sample were determined at 420 nm.

Biochemical Evaluation of Intestinal Damage.[13] Overnight-fasted rats were anesthetized with chloral hydrate. After laparotomy, a 10 cm ileal loop, situated above the ileocaecal valve, was isolated from the digestive tract by a ligature at each side. The ileal loop was treated with 30 mL of PBS (heated at 37 °C) and then flushed out with air. A 0.5 mL portion of PBS, 1% (w/v) STG, or NP-Film (5 mg) was administered to the ileum and incubated in the segments for 1 h. Then, the ileal loop was washed with 1.0 mL of PBS, and the intestinal fluid was collected. The concentration of lactate dehydrogenase (LDH) in the fluid was determined using a LDH−UV kit (Zhejiang Xinchang Kangte Bio-tech Co., Ltd.).

Tissue Histology. Histological studies were performed to evaluate the effects of NP-Film on the intestinal mucosa. NP-Film was

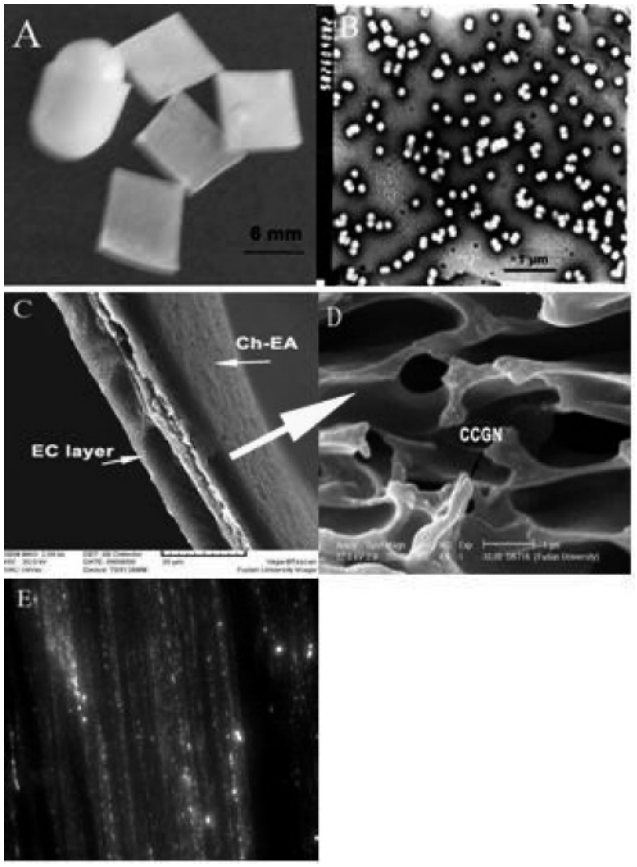

Figure 1. (A) Images of capsules containing NP-Films and a close up of NP-Films themselves. Bar represents 6 mm. (B) Transmission electron micrographs of CCGNs. Bar represents 1 μm. (C) SEM images of a cross-section of the NP-Film. Bar represents 20 μm. (D) SEM images of CCGNs dispersing in the Ch-EA layer of the NP-Film. Bar represents 1 μm. (E) Image of coumarin-6-labeled CCGNs dispersing in Ch-EA by a fluorescence microscope (6400×).

administered intragastrically to rats, and normal rats (no treatment) were used as the control. The rats were euthanized after 3 h, and their intestinal mucosa exposed to the NP-Film were excised, fixed in formalin, sectioned, and stained using hematoxylin and eosin.

Results and Discussion

Morphology. Images of the capsules that encapsulate the NP-Film composed of CCGNs and the bilaminated film are shown in Figure 1A. TEM photographs exhibit that the resulting nanoparticles are spherical and separate from each other (Figure 1B). The prepared NP-Film was flexible, and its thickness was about 20 μm (Figure 1C). Ch-EA was easily laminated onto the hydrophobic layer, and then a perfect binding was achieved, as was demonstrated by SEM of the film cross-sections. The mucoadhesive layer displayed many porous structures in which solid, spherical CCGNs (Figure 1D) were dispersed. Coumarin-6, the small lipophilic dye, could label CCGNs because of its hydrophobic core. Coumarin-6-labeled CCGNs dispersing in the NP-Film could also be seen by a fluorescence microscope (Figure 1E).

Preparation of CCGNs. A redox system combining free NH_2 groups of carboxylation chitosan and APS initiated the graft polymerization of carboxylation chitosan and methyl methacrylate.[14] Because of the amphiphilic property of the grafted polymer, nanoparticles could spontaneously be formed in aqueous medium.

Table 1. Particle Size, Surface Charge, Theoretical Loading, and Encapsulation Efficiency of Different Nanoparticles

formulations[a]	diameter (nm ± SD)	PDI[b]	zeta potential (mV)	theoretical loading (%)	encapsulation efficiency (%)
1[c]	288.5 ± 7.1	0.002	−57.04 ± 3.43	10	97.33
2[d]	274.4 ± 15.0	0.021	−50.21 ± 0.56	10	85.26
3[e]	233.4 ± 7.3	0.011	−41.03 ± 1.75	10	81.19
4[f]	169.0 ± 10.0	0.136	−7.07 ± 0.27	10	10.00
2[d]	274.4 ± 15.0	0.021	−50.21 ± 0.56	20	76.60
2[d]	274.4 ± 15.0	0.021	−50.21 ± 0.56	5	100.00

[a] The weight ratio of carboxylation chitosan to methyl methacrylate. [b] The PDI. [c] The weight ratio of carboxylation chitosan to methyl methacrylate was 3:1. [d] The weight ratio of carboxylation chitosan to methyl methacrylate was 1:1. [e] The weight ratio of carboxylation chitosan to methyl methacrylate was 1:3. [f] The carboxylation chitosan was not added.

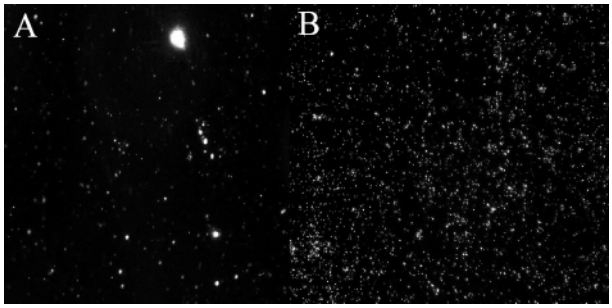

Figure 2. Morphological changes of coumarin-6-labeled CCGNs in simulated GI conditions by a fluorescence microscope. (A) CCGNs in the simulated gastric fluid (6400×). (B) CCGNs in the simulated intestinal fluid (6400×).

Effect of APS on CCGNs. Increasing the concentration of APS from 0.01% to 0.05% with a fixed concentration of methyl methacrylate and carboxylation chitosan at definite temperature, the diameter of the resulting nanoparticles decreased from 676 to 280 nm. This was because higher APS concentration increased the number of the radicals, resulting in a reduction of the molecular weight of the copolymers. In one of the previous studies, a strong correlation between particle diameters and molecular weights was observed for sulfopropyl-methacrylate copolymer nanoparticles.[15] Hence, it is very likely that the increase of initiator concentration contributed to the smaller nanoparticle size.

Effect of Monomer Ratios on CCGNs. Table 1 shows that the surface charge and diameter of CCGNs are dependent on the portions of the carboxylation chitosan. With the increase of carboxylation chitosan, the surface charge of CCGNs decreased. The reason was that carboxyl groups, which concentrated on the particle surface, were in the form of $-COO^-$ in water. By increasing carboxylation chitosan, the particles possessed more negative zeta potential due to the increase of carboxyl groups.

Encapsulation Efficiency. CCGNs had high encapsulation efficiency for insulin, reaching as high as 100%, while that of PMMA was only 10% (Table 1). The high encapsulation efficiency of CCGNs was related to the affinity of the positively charged insulin with the negatively charged carboxyl groups on the surface of nanoparticles. The encapsulation efficiency for insulin was also significantly influenced by the initial insulin concentration (Table 1). The lower theoretical loading of insulin led to higher encapsulation efficiency.

Stability of Nanoparticles in Different Simulated GI Conditions. Figure 2 shows that the coumarin-6-labeled nanoparticles tend to aggregate in the gastric medium while they separate from each other in the intestinal medium. Since the nanoparticles had carboxyl groups, under strong acidic condi-

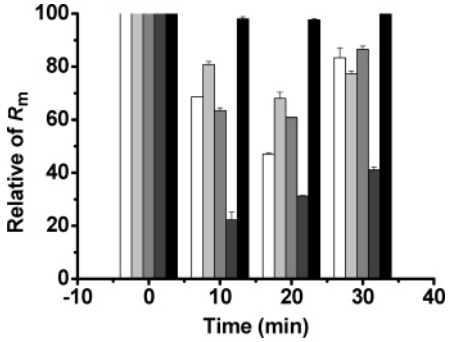

Figure 3. Effect of CCGNs on the membrane resistance (R_m) (mean ± standard deviation (SD), $n = 3$). White represents CCGNs in which the weight ratio of carboxylation chitosan to methyl methacrylate was 3:1. Light gray represents CCGNs in which the weight ratio of carboxylation chitosan to methyl methacrylate was 1:1. Gray represents CCGNs in which the weight ratio of carboxylation chitosan to methyl methacrylate was 1:3. Dark gray represents STD. Black represents double-distilled water.

tions, most of carboxyl groups of CCGNs were in the form of −COOH. Therefore, the charges of CCGNs disappeared, which led to the aggregation of nanoparticles due to losing the repulsion forces between particles. In contrast, in the intestinal medium, almost all carboxyl groups of CCGNs were in the form of $-COO^-$. So the electrostatic repulsive forces of CCGNs increased, resulting in the separation of the nanoparticles.

Effect of CCGNs on the R_m. The R_m was slightly different when water was added (negative control). This value increased 3 times when STG, which opened the tight junction of the intestine, was used as the positive control. It decreased at first and then increased in the presence of nanoparticles (Figure 3).

The intactness of the tight junctions was linked to the presence of Ca^{2+} and Mg^{2+}. The reduction of extracellular Ca^{2+} concentration can result in an opening of the tight junctions, leading the R_m to decrease. Carboxyl groups of CCGNs might deplete Ca^{2+} from the tight junctions, and R_m decreased allowing paracellular peptide drug transport. However, the R_m increased after several minutes, indicating the viability of the cells. It is well-known that some permeation enhancers such as STG enhance the absorption of poorly absorptive drugs by causing the mucosal damage in the GI tract, and this damage is not reversible. Therefore, a transient and reversible opening of the tight junctions between the epithelial cells by CCGNs would allow for the permeation of nonabsorbable drugs into the systemic blood circulation.

Enzyme Inhibition. The activity of trypsin decreased to 25% in the presence of CCGNs. The reduced activity of trypsin might be attributed to Ca^{2+} depletion from the enzyme structure by the carboxyl groups, and Ca^{2+} played an important role in maintaining the thermodynamic stability of this enzyme.

Effect of pH on the Swelling Ratios of the Bilaminated Film. Figure 4A shows that the film displays pH-sensitive characteristics in its swelling behavior. When the pH value increased from 1.7 to 8.1, the swelling ratio decreased at first and then increased, with the lowest swelling ratio at a pH value around 6.4.

The swelling behavior of the bilaminated film was determined by the Ch-EA layer because the EC layer is hydrophobic. The Ch-EA layer was formed by chemical cross-linking of Ch with Na_2-EDTA, which contained both carboxyl and amino groups, and thus formed networks with oppositely charged structures, which could change the charge state of the ionic groups with varying pH. In the case of low pH, the dominant charges in the film were protonated amino groups; in the case of high pH, the dominant charges in the film were carboxyl groups. In these pH regions, the film swelled because of the increase in the ionic swelling pressure. The pK_a of the film might be at a pH value of about 6.4, at which most of the ionic groups were absent because of protonation of the carboxyl groups and deprotonation of the amino groups, leading to a film having a small swelling ratio.

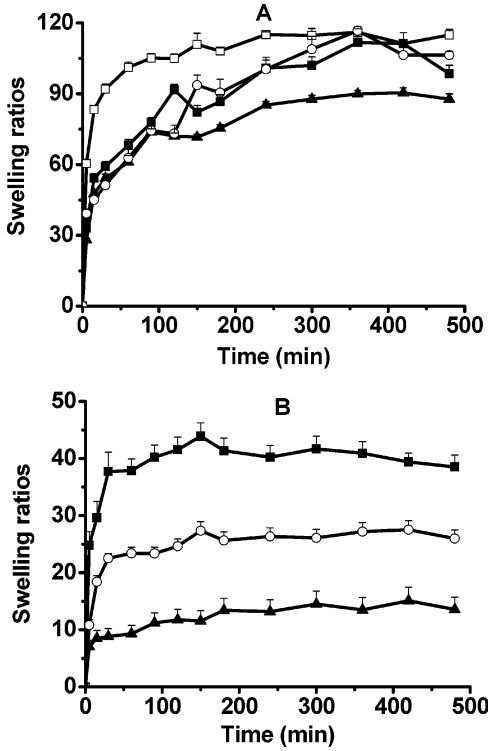

Figure 4. Swelling ratios of bilaminated film in solutions with different pH values and ionic strengths (mean ± SD, $n = 3$). (A) The swelling ratios of films in solutions with different pH values: □ 1.7; ○ 8.1; ■ 3.9; ▲ 6.4. (B) The swelling ratios of films in solutions with different ionic strengths: ■ 0.0001 mol/L NaCl; ○ 0.01 mol/L NaCl; ▲ 1 mol/L NaCl.

Effect of Ionic Strength on the Swelling Ratios of the Bilaminated Film. Figure 4B shows that the swelling ratio decreases as the ionic strength of the surrounding medium increases. The effect of electrolyte on swelling could be attributed to osmotic pressure, which resulted from the difference in ion concentration between the interior of a film network and its surrounding medium. An increase in the ionic concentration (or ionic strength) of the surrounding medium will increase the concentration gradient, which in turn would increase osmotic pressure across the boundary. Higher osmotic pressure could facilitate the diffusion of water molecules from inside the swollen film into its surrounding medium, i.e., less water retention and lower swelling ratio of the film in a high ionic strength medium is observed.[16]

Mucoadhesive Force. Figure 5 shows that the mucoadhesive force of NP-Film is high, and it is even higher than that of bilaminated films. Different mechanisms coexist for the mucoadhesion of bilaminated films, including viscosity, suitable hydration, and sufficient flexibility of the polymeric chains for entanglement with the mucosal tissue. Carboxyl groups of CCGNs had an additional effect on tissue adhesion, due to the large amount of strong hydrogen-bonding groups (−OH, −COOH) on the polymer chains.

It could also be observed that the mucoadhesive force of the NP-Film was highest in the ileum. The highest mucoadhesive

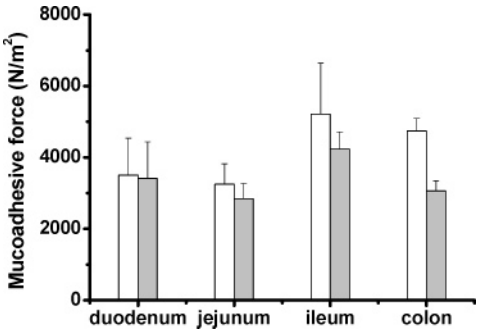

Figure 5. The mucoadhesive force of the NP-Film and the bilaminated films at different intestinal tissues (mean ± SD, $n = 4$). White represents the NP-Film, and light gray represents the bilaminated films.

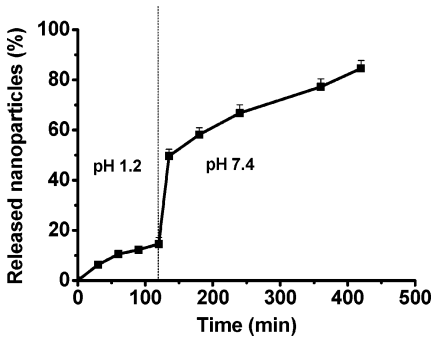

Figure 6. Release of CCGNs from the NP-Film (mean ± SD, $n = 3$). In the first 2 h, CCGNs were released in the simulated gastric fluid (pH 1.2), then they were released in the simulated intestinal fluid (pH 7.4) for 5 h.

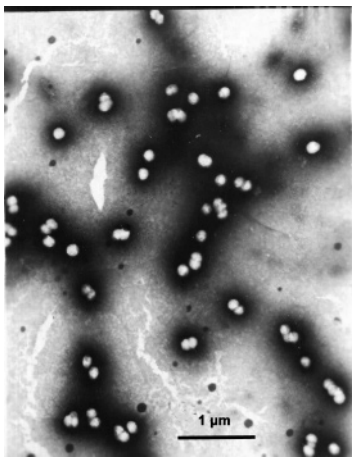

Figure 7. Morphology of the released nanoparticles in the simulated intestinal fluid. Bar represents 1 μm.

force might favor the absorption of nanoparticles because of the high number of Peyer's patches in the ileum.

Release of Nanoparticles from the NP-Film. Figure 6 shows that nanoparticles released from the NP-Film exhibit pH-sensitive behavior. In the simulated gastric medium, the release of nanoparticles was slow, while it was fast in the intestinal medium. The results might be related to CCGN states in different conditions. In the gastric condition, the aggregated CCGNs were hard to be released from the NP-Film. While in the intestinal condition, the carboxyl groups of the CCGNs were in the form of COO^-, so the electrostatic repulsive forces of the CCGNs increased, resulting in the release of nanoparticles. Figure 7 shows that the morphology of the released nanoparticles is not changed after they were released from the NP-Film in the simulated intestinal conditions.

Table 2. LDH Leakage Following PBS (control), NP-Film, and 1.0% (w/v) STG[a]

preparations	LDH leakage [U]
PBS	0.838 ± 0.047
STG	3.144 ± 0.669
NP−Film	0.893 ± 0.114

[a] Data: mean ± SD ($n = 6$).

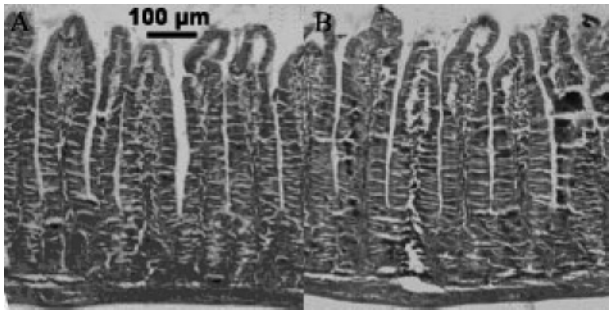

Figure 8. Histological section of (A) a control rat intestine (no treatment) and (B) rat intestine after contact with the NP-Film for 3 h. Bar represents 100 μm.

Biochemical Evaluation of Intestinal Damage. Table 2 shows the LDH leakage following a 1 h administration of the NP-Film to the ileum region. LDH was negligibly leaked into the ileal loop, which was similar to the leakage seen in the control group. In contrast, the leakage was dramatically increased by the administration of STG, indicative that STG significantly decreased the R_m. These data suggested that the ileum membrane integrity and cellular tight junctions remained mostly unchanged by the administration of the NP-Film, while STG extensively damaged the epithelial of intestinal membrane.

Tissue Histology. Histological sections of the intestinal mucosa exposed to the NP-Film for up to 3 h were examined with a light microscope and did not show any deleterious effects compared to the controls (Figure 8A (control) and B (3-h contact)).

Conclusions

The smart NP-Film possessed high mucoadhesion, pH sensitivity, enzyme inhibition, high encapsulation efficiency for hydrophilic protein drugs such as insulin, and reversible opening of the tight junction of intestinal mucosa. Therefore, the NP-Film might be a promising delivery carrier for protein drugs via oral administration.

Acknowledgment. The authors are thankful for the financial support from the Science and Technology Commission of Shanghai Municipality of China (No. 054319934).

References and Notes

(1) He, H. Y.; Guan, J. J.; Lee, J. L. *J. Controlled Release* **2006**, *110*, 339−346.
(2) Lin, Y. H.; Mi, F. L.; Chen, C. T.; Chang, W. C.; Peng, S. F.; Liang, H. F.; Sung, H. W. *Biomacromolecules* **2007**, *8*, 146−152.
(3) Dorkoosh, F. A.; Verhoef, J. C.; Borchard, G.; Rafiee-Tehrani, M.; Verheijden, H. H. M.; Junginger, H. E. *Int. J. Pharm.* **2002**, *247*, 47−55.
(4) Whitehead, K.; Shen, Z.; Mitragotri, S. *J. Controlled Release* **2003**, *88*, 37−45.
(5) Takeuchi, H.; Yamamoto, H.; Kawashima, Y. *Adv. Drug Delivery Rev.* **2001**, *47*, 39−54.
(6) Cui, F. Y.; Qian, F.; Yin, C. H. *Int. J. Pharm.* **2006**, *316*, 154−161.

(7) Bernkop-Schnürch, A.; Krajicek, M. E. *J. Controlled Release* **1998**, *50*, 215−223.
(8) Peterson, P. L. *Anal. Biochem.* **1977**, *83*, 346−356.
(9) Sakuma, S.; Sudo, R.; Suzuki, N.; Kikuchi, H.; Akashi, M.; Ishida, Y.; Hayashi, M. *J. Controlled Release* **2002**, *81*, 281−290.
(10) Sarmento, B.; Ferreira, D. C.; Jorgensen, L.; van de Weert, M. *Eur. J. Pharm. Biopharm.* **2007**, *65*, 10−17.
(11) Qian, F.; Cui, F. Y.; Yin, C. H. *Eur. Polym. J.* **2006**, *42*, 1653−1661.
(12) Yin, L. C.; Fei, L. K.; Cui, F. Y.; Tang, C.; Yin, C. H. *Biomaterials* **2007**, *28*, 1258−1266.
(13) Morishita, M.; Goto, T.; Peppas, N. A.; Joseph, J. I.; Torjman, M. C.; Munsick, C.; Nakamura, K.; Yamagata, T.; Takayama, K.; Lowman, A. M. *J. Controlled Release* **2004**, *97*, 115−124.
(14) Qian, F.; Cui, F. Y.; Ding, J. Y.; Tang, C.; Yin, C. H. *Biomacromolecules* **2006**, *7*, 2722−2727.
(15) Langer, K.; Marburger, C.; Berthold, A.; Kreuter, J.; Stieneker, F. *Int. J. Pharm.* **1996**, *137*, 67−74.
(16) Sun, G. M.; Chu, C. C. *Carbohydr. Polym.* **2006**, *65*, 273−287.

BM070339E